Chemistry & Biology
Article

Single-Molecule FRET Reveals a Cooperative Effect of Two Methyl Group Modifications in the Folding of Human Mitochondrial tRNA^{Lys}

Andrei Yu Kobitski,[1] Martin Hengesbach,[2] Salifu Seidu-Larry,[2] Kirsten Dammertz,[3] Christine S. Chow,[4] Arthur van Aerschot,[5] G. Ulrich Nienhaus,[1,6,*] and Mark Helm[2,7,*]
[1]Institute of Applied Physics and Center for Functional Nanostructures, Karlsruhe Institute of Technology, 76131 Karlsruhe, Germany
[2]Institute of Pharmacy and Molecular Biotechnology, Heidelberg University, 69120 Heidelberg, Germany
[3]Institute of Biophysics, University of Ulm, 89069 Ulm, Germany
[4]Department of Chemistry, Wayne State University, Detroit, MI 48202, USA
[5]Medicinal Chemistry, Katholieke Universiteit Leuven, Minderbroedersstraat 10 B-3000, Leuven, Belgium
[6]Department of Physics, University of Illinois at Urbana-Champaign, Urbana, IL 61801, USA
[7]Institute of Pharmacy and Biochemistry, University of Mainz, 55128 Mainz, Germany
*Correspondence: uli@uiuc.edu (G.U.N.), mhelm@uni-mainz.de (M.H.)
DOI 10.1016/j.chembiol.2011.03.016

SUMMARY

Using a combination of advanced RNA synthesis techniques and single molecule spectroscopy, the deconvolution of individual contributions of post-transcriptional modifications to the overall folding and stabilization of human mitochondrial tRNA^{Lys} is described. An unexpected destabilizing effect of two pseudouridines on the native tRNA folding was evidenced. Furthermore, the presence of m^{2}G10 alone does not facilitate the folding of tRNA^{Lys}, but a stabilization of the biologically functional cloverleaf shape in conjunction with the principal stabilizing component m^{1}A9 exceeds the contribution of m^{1}A alone. This constitutes an unprecedented cooperative effect of two nucleotide modifications in the context of a naturally occurring RNA, which may be of general importance for tRNA structure and help understanding several recently described decay pathways for hypomodified tRNAs.

INTRODUCTION

Posttranscriptional modification is a ubiquitous phenomenon observed in a great variety of different cellular RNA species, including tRNA, rRNA, mRNA, snoRNA, and miRNA (Czerwoniec et al., 2009). tRNA is the most strongly modified RNA species, accounting also for the majority of the over 100 chemically distinct nucleotide modifications known so far (Cantara et al., 2011; Czerwoniec et al., 2009). In tRNA, modifications may be roughly divided into ''functional'' modifications, which mainly govern the decoding properties of the anticodon, and ''structural'' modifications, which are mostly chemically simple modifications, such as pseudouridines or methylated nucleotides (Helm, 2006; Motorin and Helm, 2010). A telltale of the structural modifications is their frequent occurrence at nucleotides involved in tertiary interactions that govern the intricate folding of the tRNA core. It is due to these tertiary interactions that the well-known cloverleaf secondary structure does indeed fold into a compact and very stable three-dimensional L-shape. The multitude of posttranscriptional modifications occurring in the tRNA core presents a complex problem to analyze as they are thought to function as a complex network whose collective effect lends thermodynamic, biochemical, and metabolic stability to the modified tRNA (Chernyakov et al., 2008; Engelke and Hopper, 2006; Helm, 2006; Motorin and Helm, 2010). It appears that the absence of a single modification from this ensemble does not necessarily produce a detrimental effect, since the majority of studies of mutants defective in a single modification have failed to yield a significant effect in either structure or function (Björk, 1995; Jackman et al., 2003; Kotelawala et al., 2008). tRNAs of identical genomic sequence but differential posttranscriptional modifications pattern have been termed modivariants (Madore et al., 1999). Significant effects of modivariants lacking single modifications have only recently been observed in a few isolated cases (Alexandrov et al., 2005; Anderson et al., 1998). More importantly, investigations into the network have demonstrated that severe phenotypes typically only occur in the absence of two or more structural modifications from a canonical tRNA (Alexandrov et al., 2006; Engelke and Hopper, 2006). Measurements of biophysical parameters as a basis for the understanding of core modifications have initially been conducted by comparative studies of tRNA samples that were unmodified in vitro transcripts and fully modified native tRNAs (Derrick and Horowitz, 1993; Helm et al., 1998; Perret et al., 1990; Sampson and Uhlenbeck, 1988). Numerous studies have been conducted on tRNA fragments such as anticodon-stem loops, which are amenable to chemical synthesis including various modifications (for review, see Helm, 2006). Fewer reports concern full-length tRNAs that are either hypomodified with respect to a single modification, or, which contain only a single modification (Helm et al., 1999; Kobitski et al., 2008; Pütz et al., 1994; Voigts-Hoffmann et al., 2007). So far, comprehensive studies are lacking on modivariant sets containing permutations of the modifications present in the structural core of tRNAs. This is related to the demanding task of synthesizing these modivariants in sufficient amounts for biophysical studies.

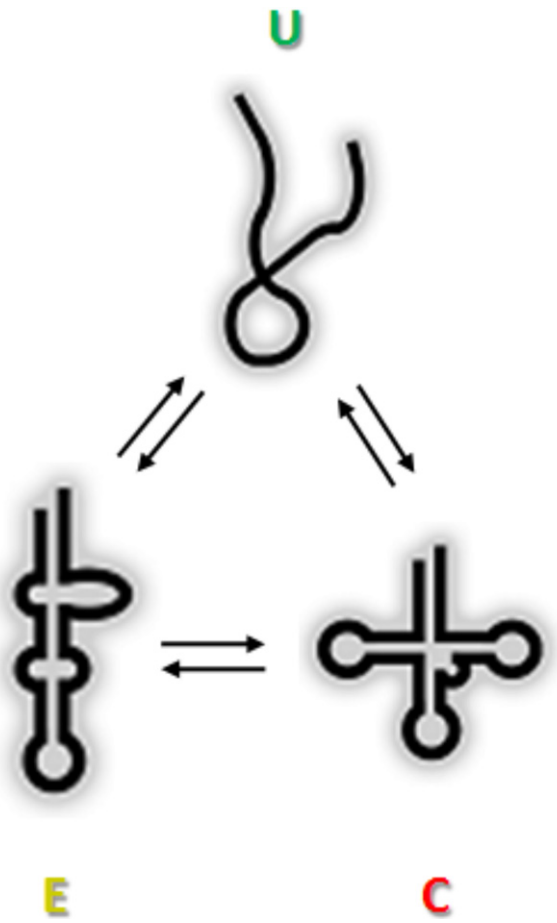

Figure 1. Schematic Representation of the Folding of Human Mitochondrial tRNA^{Lys}

Three thermodynamically stable conformations that represent the unfolded sate (**U**), the extended hairpin state (**E**), and the functional cloverleaf-based state (**C**) are depicted.

In the present work, we approach this problem by a combination of sophisticated chemical and biochemical RNA syntheses in conjunction with single-molecule Förster Resonance Energy Transfer (smFRET) studies. FRET from an excited donor fluorophore to an acceptor fluorophore depends on the inverse sixth power of the interdye distance and, because fluorescence emission can be detected with excellent time resolution, smFRET is an attractive method for the observation of distance variations between two dye-labeled domains of a given RNA (for review, see Helm et al., 2009). Here, we mate smFRET with the combinatorial use of splint ligations. Splint ligations of chemically synthesized RNA fragments containing defined sets of modifications and fluorescent dyes permits the efficient and versatile synthesis of modivariants for single molecule thermodynamic analysis of conformational states (Hengesbach et al., 2008; Kurschat et al., 2005). Previous studies have identified human mitochondrial tRNA^{Lys} as an object well suited for this kind of investigation. As sketched in Figure 1, three thermodynamically stable conformations, denoted as **U** (for "unfolded"), **E** (for "extended hairpin"), and **C** (for fully folded "cloverleaf" structure), have been observed for this tRNA (Kobitski et al., 2008; Voigts-Hoffmann et al., 2007). The relative populations of these states are governed by the counterion concentration; in addition, the equilibrium was shown to be shifted toward the cloverleaf by the presence of m^{1}A9. A detailed study of the related biophysical parameters was possible because both conformations are of similar free energy and thus present in measurable proportions in equilibrium, which, in addition, can be efficiently influenced through variation of the multivalent ion concentration (Kobitski et al., 2008). Here we show that this framework is also suitable to investigate the interactions of multiple core modifications of tRNA^{Lys}, i.e., m^{1}A9, m^{2}G10, and pseudouridines 27 and 28. Notably, it was found that m^{2}G10 alone did not significantly influence tRNA folding, but did show a pronounced cooperative effect with the other methyl group modification of the core, m^{1}A9. This observation presents a first biophysical basis for the emerging notion that structural core modifications in tRNA act as a concerted network for the fine-tuning of structural features rather than as a binary all-or-nothing effect.

RESULTS

Using a combinatorial approach described below, a total of eight human mt tRNA^{Lys} modivariants containing m^{1}A9, m^{2}G10, Ψ27, and Ψ28 modifications in various compositions were synthesized by splint ligation (Hengesbach et al., 2008; Kurschat et al., 2005; Voigts-Hoffmann et al., 2007), and their conformational states were analyzed by smFRET. The position of the nucleotide modifications and the synthesis scheme are shown in crystal structure of tRNA^{Phe} in Figure 2. Figure S1 (available online) provides atomic details on the relative orientation of the methylgroups in m^{1}A and m^{2}G.

In Vitro Reconstruction of Modivariants of Human Mitochondrial tRNA^{Lys}

Modivariants of tRNA^{Lys} suitable for smFRET analysis contain up to six modified nucleotides at defined positions, including the four naturally occurring core modifications and the two fluorescent dyes Cy3 and Cy5 which form a FRET pair. We have addressed this challenge by devising a construction-kit approach which uses splint ligation to assemble up to four synthetic RNA fragments in a one-pot reaction. For the introduction of modifications, selected fragments are replaced with such of identical sequence but carrying modifications incorporated by solid-phase phosphoramidite chemistry. Through permutations of fragments, a variety of different modivariants become accessible from a limited pool of fragments, whose length is dictated by the position of natural modifications and suitable attachment points for the FRET dyes. The latter have been previously established based on the crystal structure of tRNA^{Phe} (Shi and Moore, 2000) and validated for tRNA^{Lys} by showing that the resulting tRNAs are still substrates for modification enzymes and RNase P (Voigts-Hoffmann et al., 2007). A particular challenge arose from the close proximity of the Cy3 dye at position 4 and the modifications at positions 9 and 10. Biochemical restrictions arising from the substrate specificity of T4 DNA ligase necessitated a ligation site between nucleotides 5 and 6 and, congruously, the ligation of a Cy3-containing fragment longer than

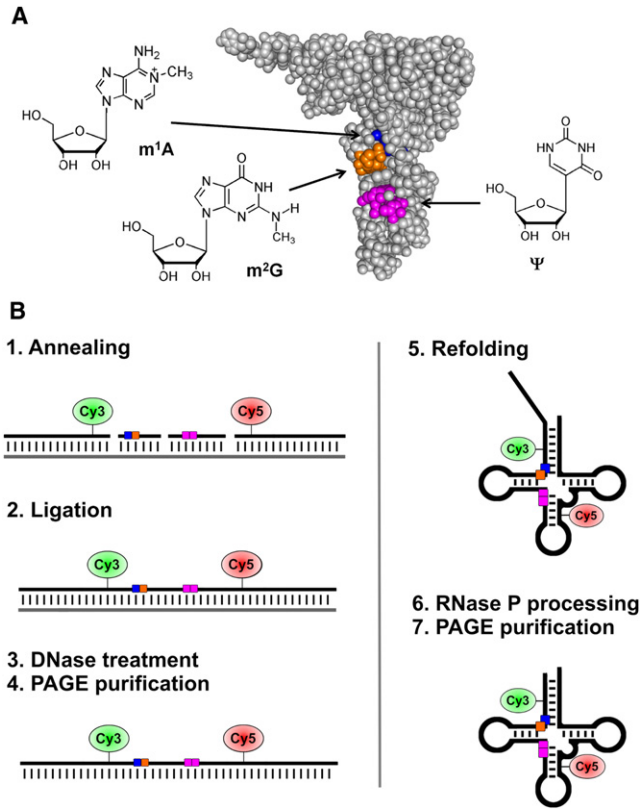

Figure 2. Introduction of Modified Nucleotides into Human Mitochondrial tRNA^{Lys}

(A) m^{1}A9 (blue), m^{2}G10 (orange), and Ψ27Ψ28 (pink) are represented on the three-dimensional tRNA structure of tRNA^{Phe} from yeast (Shi and Moore, 2000).

(B) Synthesis of FRET-labeled tRNA modivariants by combination of chemical synthesis and splint ligation. Fragments obtained by solid-phase synthesis are phosphorylated and annealed onto a full-length complementary splint (1). The fragments may contain the natural modifications m^{1}A (blue), m^{2}G (orange), and pseudouridine (pink), as well as fluorophores of a FRET pair, e.g., Cy3 and Cy5 as indicated. Ligation sites are recognized by T4 DNA ligase as "nicks" in the resulting DNA: RNA duplex and repaired (2). The DNA splint is removed by DNase treatment (3) and, after purification by PAGE (4), the resulting tRNA precursor is refolded in the presence of Mg^{2+} ions (5). The leader sequence is cleaved off by the catalytic RNA component of bacterial RNase P, and the final modivariant is isolated after renewed purification by PAGE.

See also Figures S1 and S2.

five nucleotides. As shown in Figure 2B, modivariants including either m^{1}A9 or m^{2}G10 were therefore synthesized as pre-tRNAs carrying a 12 nt long leader sequence, and then catalytically cleaved by RNase P RNA to yield the final modivariants of proper tRNA size.

Sequential Incorporation of m^{1}A and m^{2}G Phosphoramidites

The incorporation of *N1*-methyl-adenosine into RNA by conventional phosphoramidite chemistry is particularly challenging, since standard deprotection typically includes alkaline treatment in aqueous solution, resulting in a Dimroth rearrangement of m^{1}A to m^{6}A. This limitation can be overcome by working under strictly anhydrous conditions as with the use of a 2 M solution of ammonia in dry methanol. The latter gives a clean removal of the more labile chloroacetyl protective group specifically developed for m^{1}A protection (Mikhailov et al., 2002). While many base methylated ribonucleosides have been incorporated before into oligo(ribo)nucleotides (Höbartner et al., 2003), the combination of m^{1}A with different modifications was not attempted so far. Hence, judicious choice of the protecting groups was necessary. However, as Höbartner et al. (Höbartner et al., 2003) achieved straightforward deprotection of the p-nitrophenylethyl (NPE) group using 1 M tetrabutylammoniumfluoride (TBAF), we opted for their strategy combining their 2′-O-[(triisopropylsilyl)oxy] methyl (TOM) protected O^6-NPE-m^{2}G phosphoramidite with our chloroacetyl protected m^{1}A. The absence of side reaction products for the isolated material (e.g., Dimroth rearrangement) was verified by ESI-TOF mass spectrometry (MS/MS of the methylated base fragment shown in Figure S2).

smFRET Measurements of tRNA^{Lys} Modivariants

To compare the folding ability of prepared constructs under near-physiological salt conditions (pH 7.4, 1 mM Mg^{2+}, 1 mM Ca^{2+}, 100 mM K^+), smFRET measurements on freely diffusing tRNA molecules were conducted on a confocal microscope with single-molecule sensitivity (Kobitski et al., 2007, 2008; Kuzmenkina et al., 2006; Rieger et al., 2010). Donor and acceptor signal of ~1 ms fluorescent bursts were collected in separate spectral channels with 100 μs time resolution. Moreover, by using alternating green/red laser excitation (Kapanidis et al., 2004) within the 100 μs time bin with a 70% duty cycle for green excitation, only those molecules with properly functioning donor and acceptor dyes were selected. Then, FRET efficiencies of individual bursts were calculated by ratiometric analysis of donor and acceptor intensities, corrected for background, spectral cross-talk, and differences in the detection efficiencies. Compiled histograms of FRET efficiency values from several hundreds of molecules are presented in Figure 3 for the Kwt, KΨΨ, Km^{2}G, Km^{1}A, Km^{1}Am^{2}G, and Kcore constructs. Three previously established conformational states, ***U***, ***E***, and ***C*** (Kobitski et al., 2008; Voigts-Hoffmann et al., 2007), are also recognized in the newly studied probes. The influence of m^{1}A9, which has been described before (Kobitski et al., 2008; Voigts-Hoffmann et al., 2007), can be clearly observed by comparing Kwt to Km^{1}A, which shows a significant population of the functional ***C*** conformation. The introduction of m^{2}G10 into the completely unmodified Kwt leads to the modivariant Km^{2}G, which does not, however, show an appreciable ***C*** population. Nevertheless, the ***E*** state becomes slightly better stabilized with respect to the ***U*** state. By introducing m^{2}G into Km^{1}A (which is identical to introducing of m^{1}A into Km^{2}G) further decrease in the ***U*** population and some increase of the ***C*** population could be noticed. Further surprising observations concern modivariants containing pseudouridine. The most properly folded construct is the Km^{1}Am^{2}G modivariant, which shows the highest population of the functional conformation ***C***, while the most modified modivariant Kcore, which contains all four modifications, has a significantly reduced ***C*** population. Likewise, the ***C*** population is almost absent in the KΨΨ modivariant with respect to the Kwt. Thus, the two pseudouridines at positions 27 and 28 obviously have a destabilizing influence

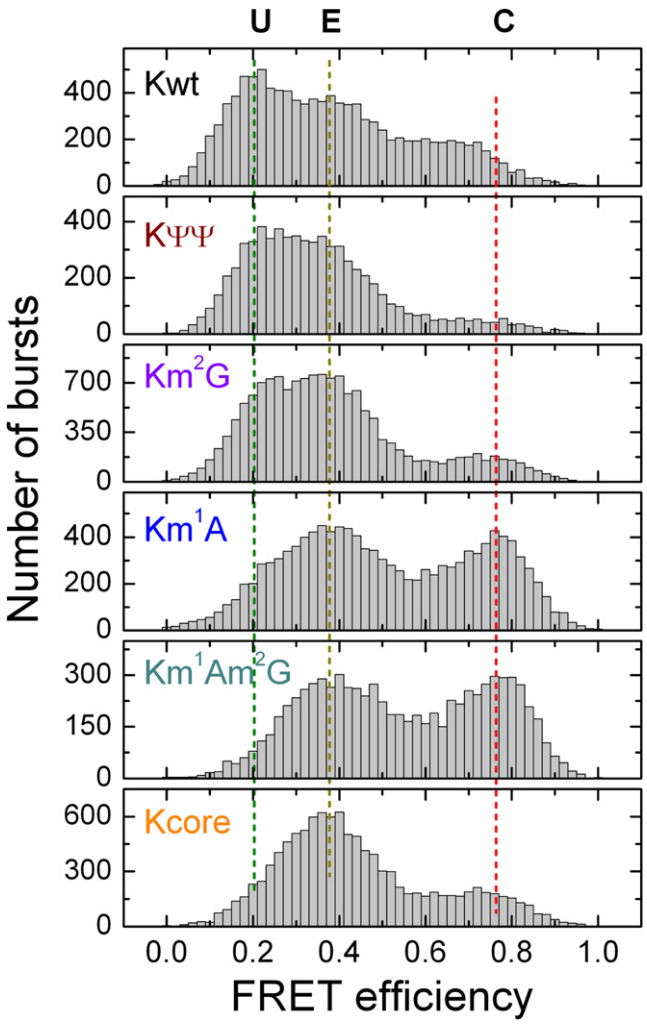

Figure 3. Detection by smFRET of Conformational States in Modivariants of tRNA^{Lys}

Histograms of FRET efficiency values, *E*, measured on freely diffusing Kwt, KΨΨ, Km^{2}G, Km^{1}A, Km^{1}Am^{2}G, and Kcore tRNA molecules in physiological buffer. Dotted lines depict the approximate average FRET efficiencies of the ***U*** (green), ***E*** (dark yellow), and ***C*** (red) states.

on the cloverleaf structure in this particular tRNA, favoring the extended hairpin instead.

Mg^{2+}-Dependent Folding of tRNA^{Lys}

To obtain a thermodynamic basis for these observations, populations in the modivariants have been analyzed in detail as a function of Mg^{2+} ion concentration. The quantitative analysis of the respective energy landscape changes were performed within the thermodynamic framework developed in our previous publications (Kobitski et al., 2007, 2008). Thus, FRET efficiency histograms taken at up to 20 different Mg^{2+} concentrations in the range from 0.0063 up to 400 mM for each construct were fitted by a superposition of the ***U***, ***E***, and ***C*** state distributions (Figure S3). In Figure 4, the fractional subpopulations of the ***U***, ***E***, and ***C*** states of the Kwt, Km^{2}G, KΨΨ, Km^{1}A, Km^{1}Am^{2}G, and Kcore constructs are plotted as a function of the counterion concentration. For all samples, a drop of the ***U*** state is accompanied by a concomitant rise of the ***C*** state with increasing Mg^{2+} concentration. At high Mg^{2+} ion concentration the ***C*** state becomes dominant within the titration range for all constructs except KΨΨ. The ***E*** state subpopulation behaves, however, differently for the constructs without the m^{1}A9 modification and the constructs containing it. Thus, at low Mg^{2+} concentration the ***E*** state of Km^{1}A, Km^{1}Am^{2}G, and Kcore modivariant is noticeably stabilized over the ***U*** state, while for Kwt, Km^{2}G, and KΨΨ, this stabilization is cation dependent and occurs above ≈0.5 mM Mg^{2+}, i.e., already at physiological concentrations.

To extract the free energy parameters, we have applied a thermodynamic analysis of the fractional population changes that has been thoroughly discussed elsewhere (Kobitski et al., 2008). In brief, the model includes altogether six states, three states, U_0, E_0, and C_0, which represent the "Mg-free" and three more states, U_{Mg}, E_{Mg}, and C_{Mg}, which represent the "Mg-bound" states of the ***U***, ***E***, and ***C*** conformations. To describe the changes of the "Mg-bound" state populations as a function of ion concentration, the free energies of the E_{Mg} and C_{Mg} states were referenced to the U_{Mg} state and modeled empirically by a Hill-like equation, $\Delta G(\text{ion}) = \Delta G^\circ + n\,RT\ln([\text{ion}])$. Furthermore, the free energies of the E_0 and C_0 states, ΔG^0_{UE} and ΔG^0_{UC}, were also referenced to the U_0 state and the relative populations of all states was described by Boltzmann statistics. Finally, the fractional populations of the respective conformations were expressed as a sum of the "Mg-free" and "Mg-bound" state populations and fitted to the experimental data. The results of the fit are presented in Figure 4 as lines; the values of n and ΔG° are given in Table S1.

The overall good fits of the thermodynamic model to the single-molecule experimental data enable extraction of various conformation-pure thermodynamic parameters, especially, the free energy changes, $\Delta\Delta G$, of the folded conformations ***E*** and ***C*** with respect to the ***U*** state, or to each other, respectively. The corresponding dependencies of $\Delta\Delta G$ as a function of Mg^{2+} concentration are presented for Km^{1}A, Km^{2}G, and Km^{1}Am^{2}G in Figure 5A, and for KΨΨ and Kcore in Figure 5B; Kwt is shown in both panels of Figure 5 for comparison. A value above the zero line indicates a shift of the equilibrium to the left side, a value below zero indicates a predominance of the population on the right side of the equilibrium arrows, and a zero value corresponds to equal proportions of both of the respective conformations. The progressing folding of all tRNA modivariants into the more compact ***E*** and ***C*** conformations is reflected by a monotonic decrease of $\Delta\Delta G_{UE}$ and $\Delta\Delta G_{UC}$ with increasing ion concentration.

In Figure 5, the stabilization of a modivariant relative to another is reflected by the distance of the respective lines from one another at a given Mg^{2+} concentration. Thus, by following the relative position of a pair of modivariants lines, it is immediately apparent, that the relative stabilization afforded by a given modification is strongly dependent on the Mg^{2+} concentration. For example, when following the blue (Km^{1}A) and green (Km^{1}Am^{2}G) lines in the middle panel of Figure 5A, a crossover point near physiological Mg^{2+} concentrations around 0.3 mM defines a low ion range (0–0.3 mM), in which the m^{1}A modification alone stabilizes the ***C*** over the ***U*** conformation less efficiently than do the joint methylations. This situation is reversed above physiological Mg^{2+} concentrations.

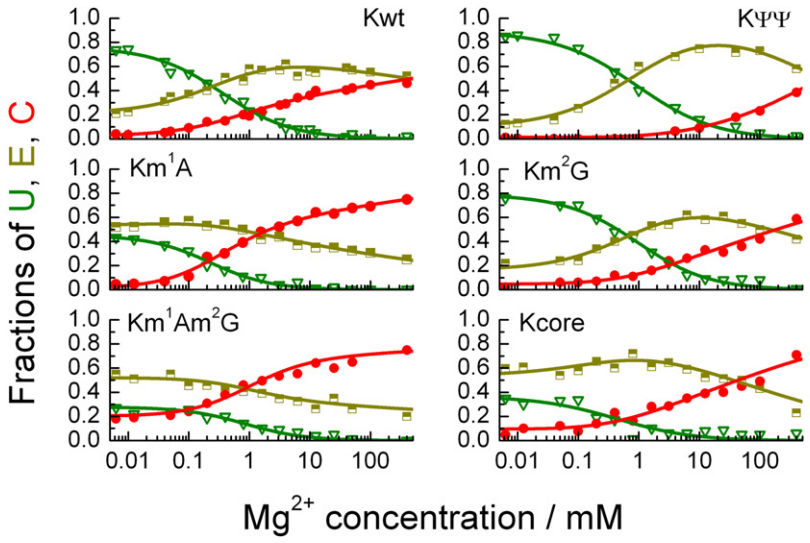

Figure 4. Mg^{2+} Dependence of the Fractional Populations in Modivariants of $tRNA^{Lys}$

Fractional populations of the ***U*** (green triangles), ***E*** (dark yellow squares), and ***C*** (red dots) states have been determined at the indicated concentrations of Mg^{2+}. Lines represent results from fitting the data with the thermodynamic model discussed in the text. See also Figure S3 and Table S1.

A Dominant m^1A Interacts Cooperatively with m^2G in tRNA Folding

Clearly, for all modivariants containing the m^1A9 modification, i.e., Km^1A, Km^1Am^2G, and Kcore, the ***C*** state is the dominant conformation, stabilized by ~4 kJ/mol with respect to the ***E*** state of the Kwt construct already at low ion concentrations. The other methyl modification, m^2G10, is slightly destabilizing for the ***E*** state as comparison of Km^2G and Kwt shows. Notably, the ***C*** state is only slightly stabilized in Km^1A and Km^2G modivariants, but is significantly stabilized by ~7 kJ/mol al low ion concentration for the joint m^1A9 and m^2G10 modification. Nevertheless, at physiologically relevant ion concentrations (shown as shaded areas in Figure 5), the stabilization of the ***E*** and ***C*** states with respect to the unfolded state and to each other is governed by conformation-specific interactions of the RNA with ions. Thus, the m^2G10 modification is more lipophilic and therefore presumably interferes with ion uptake upon tRNA folding, so, the ***E*** and ***C*** states of Km^2G become less stabilized at intermediate and high ion concentrations than in Kwt. In contrast, the m^1A9 modification of Km^1A does not affect ion uptake upon folding into both the ***E*** and the ***C*** states. For the joint methyl modifications, the interference effect is again largely present. Concerning the double pseudouridine modification, both the ***E*** and the ***C*** states are significantly destabilized by ~2 kJ/mol in the KΨΨ modivariant. Comparing the Kwt and Kcore constructs, a significant stabilization of the ***E*** and ***C*** states is observed for Kcore at low ion concentrations, while the stabilization effect becomes largely obscured at high concentration due to the interference of the modifications with the ion uptake upon folding. Altogether, this clearly shows that m^1A is the most important structural modification in this tRNA, whose effect cannot be emulated by any other of the native modifications. Additional modifications have only a secondary effect, modulating the stabilization afforded by m^1A.

A conformation-dependent interplay between modification-induced stabilization/destabilization and ion interference effects is reflected in the behavior of $\Delta\Delta G_{EC}$ as a function of Mg^{2+} concentration (Figure 5). Thus, in the physiologically relevant range of divalent ion concentrations, a direct comparison of Kwt and Km^2G (shaded areas in the middle panel of Figure 5) reveals that the m^2G modification alone does not stabilize the ***C*** conformation with respect to the ***E*** state (~0 kJ/mol at 1 mM Mg^{2+}), whereas Km^1A shows a relative stabilization of ~2.5 kJ/mol. The largest stabilization of the ***C*** state with respect to the ***E*** state, namely, by ~3 kJ/mol, is observed for the Km^1Am^2G modivariant. Thus, the stabilization afforded by the combined action of m^1A and m^2G exceeds the effect of either modification alone, and this difference defines a cooperative effect of ~0.5 kJ/mol.

DISCUSSION

Posttranscriptional base modifications enrich the chemical properties of nucleic acids and, in some cases, govern the folding of an RNA molecule into a functional conformation (Helm, 2006). So far, detailed investigations have suffered from the need to synthesize sizable amounts of modivariant samples for biophysical studies like NMR or UV melting. While NMR spectroscopy is under certain conditions suited to analyze molecular dynamics and to distinguish several conformations in an ensemble, the size of a tRNA and the magnitude of the structural rearrangements observed here make this a very difficult challenge. The strength of the present study lies in the mating of our versatile "modivariant construction kit" with smFRET measurements. The synthetic approach allows the synthesis of very small amounts of FRET-labeled tRNA modivariants, which would otherwise be difficult to characterize biophysically for lack of sufficient material. A particular strength of the smFRET technique is the distinction of different conformations present in an ensemble. This has previously allowed us to demonstrate that the m^1A9 modification significantly facilitates the folding of human mitochondrial $tRNA^{Lys}$ into the canonical cloverleaf-based L-shape (Helm et al., 1999), to the point where its absence prevents significant population of the ***C*** state under physiological concentrations of Mg^{2+} ions (Kobitski et al., 2008; Voigts-Hoffmann et al., 2007). Here, we have investigated modivariants containing three additional modifications in the core of $tRNA^{Lys}$ molecule, namely, m^2G10, Ψ27, and Ψ28. The apparent destabilization by the pseudouridines of the native tRNA structure at the expense of the unusual ***E*** state was unexpected and demands further investigation in different tRNAs. The secondary structure in the immediate vicinity of the pseudouridines, as deduced from earlier structural probing experiments (Helm et al., 1998, 1999), is similar in the ***E*** and ***C*** conformation and,

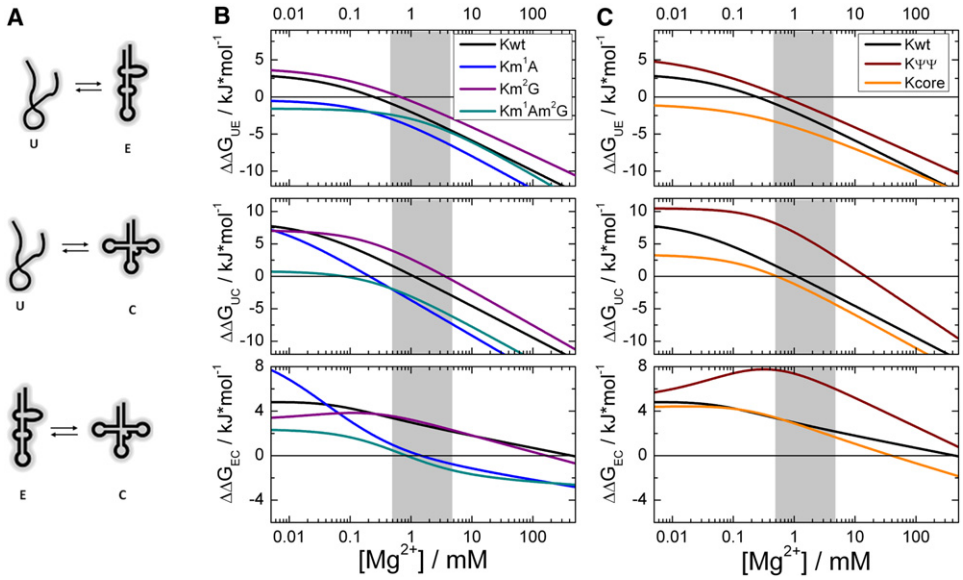

Figure 5. Thermodynamic Comparison of Three Structural Equillibria as a Function of Mg^{2+} Concentration

(A) The complex equilibrium shown in Figure 1 was broken down to the U ↔ E (upper panel), U ↔ C (middle panel), and E ↔ C (lower panel) transitions. Differences in folding free energy, ΔΔG, as a function of Mg^{2+} concentration for the U ↔ E (upper panel), U ↔ C (middle panel), and E ↔ C (lower panel) transitions of the Km^1A, Km^2G, Km^1Am^2G (B), and KΨΨ and Kcore (C) constructs are plotted; Kwt $tRNA^{Lys}$ is included in both (B) and (C) panels for comparison. The shaded area marks the region of physiologically relevant concentrations of Mg^{2+} ions. A value above the zero line indicates a shift of the equilibrium to the left side, a value below zero indicates a predominance of the population on the right side of the equilibrium arrows, and a zero value corresponds to equal proportions of both of the respective conformations. The stabilization of a modivariant relative to another is reflected by the distance of the respective lines from one another at a given Mg^{2+} concentration.

thus, does not readily yield a satisfying explanation. Possibly, structural dynamics of the anticodon domain occurring on a smaller scale, i.e., not including the rearrangements of entire domains (Helm et al., 1998), may be involved.

Our results underscore once more the outstanding importance of m^1A9 in this particular tRNA, since none of the modivariants lacking m^1A shows significant populations of the functional cloverleaf conformation at physiological concentrations of Mg^{2+} ions. It is unclear at this point if this importance applies to other mitochondrial tRNAs as well (e.g., mt $tRNA^{Asp}$) (Messmer et al., 2009a, 2009b). With the exception of the noncanonical $tRNA^{Ser}$ isoacceptors, all purines at position 9 are *N1*-methylated in all mammalian mitochondrial tRNA molecules hitherto known (Juhling et al., 2009). This suggests either a particular importance of this modification, or the action of promiscuous methyltransferases with low substrate specificity. Our own attempts to answer this question have so far been hampered by the fact that other mitochondrial tRNAs investigated in our lab, e.g., $tRNA^{Leu(CUN)}$, do not seem to display the delicately balanced equilibrium between the **E** and the **C** conformation (Hengesbach et al., 2010 and M. Hengesbach and M. Helm, unpublished data), which, in turn, makes $tRNA^{Lys}$ such a favorable object to study by smFRET.

Interestingly, the effect of nucleotide methylations in the shaping of tRNA structure indeed contains elements of both stabilization and destabilization. Thus, the methyl group in positions 1 of adenine blocks Watson-Crick base-pairing and selectively destabilizes the secondary structure of the ***E*** state. On the other hand, the same methyl group introduces a positive charge (Helm, 2006) and, thereby, may partially screen the negative charge of an RNA backbone. The latter becomes more important in the case of high negative charge density in regions with compact tertiary structure. However, such positive charge may also affect cation uptake upon folding. Therefore, the net effect of this and other modifications is determined by the interplay between conformation-dependent secondary structure destabilization, possible tertiary structure stabilization and interaction with ions.

The methyl group of m^2G may adopt an s-trans rotamer conformation without thermodynamic penalty (Rife et al., 1998), leaving the base-pairing properties unchanged. Although the increased lipophilicity of the m^2G modification is thought to reinforce base stacking interactions in helices, NMR and UV-melting studies of helices and tetraloops by Rife et al. (1998) did not show any stabilizing effect of m^2G. On the other hand, Micura et al. (2001) investigated the distribution of a self-complementary oligomer between a hairpin loop and a duplex structure, thereby observing a stabilization of the duplex structure by m^2G. This latter observation argues for a stabilizing effect of m^2G in helices. In the present case, stabilization by stacking may possibly be offset by the deficit in ion uptake of this modification. One may hypothesize, that the observed cooperative effect of m^2G and m^1A results from interplay of these bases in the particular structural context of the tRNA core (see Figure 1A). The cooperative effect is likely mediated by other participating nucleotides, since the nucleobases of residues 9 and 10 do not directly interact in tRNA structures, and the methylation sites are situated at opposing ends of the dinucleotide (see Figure S1).

Table 1. tRNA Derivatives Synthesized by Splint Ligation

tRNA Derivatives	I	II	III	IVa	IVb	IVc	V	Vb	VI
Kwt	●								●
preKm1A			●	●			●		●
preKm2G			●		●		●		●
preKm1Am2G			●			●	●		●
KΨΨ		●						●	●
preKcore			●			●		●	●

The oligoribonucleotides employed are given in roman numbers.

Research into the structural and metabolic effects of tRNA core modifications has recently received renewed interest, in part, due to the discovery of several degradation pathways which act as quality surveillance systems, eliminating hypomodified or otherwise structurally destabilized tRNA (Alexandrov et al., 2006; Chernyakov et al., 2008; Kadaba et al., 2004, 2006). Our description of a cooperative effect of two modifications may provide a thermodynamic basis for these observations. Possibly, only a few selected modifications, such as, e.g., m^1A58 in yeast occupy crucial positions in the tRNA tertiary interaction network (Anderson et al., 1998, 2000), while the others confer stability to the tRNA core through a cooperative network. Although cooperativity between multiple modifications may conceivably be even harder to analyze, the approach presented here should be suitable to address even more complex systems. Since the construction of various modivariants and their analysis by smFRET have been well established, the challenge will be to identify tRNA species in which multiple structural states are present in significant proportions and their relative populations are influenced by the respective modifications.

SIGNIFICANCE

The ensemble of modifications in the structural core of tRNAs is thought to fine-tune the structural stability and flexibility that is required for tRNA participation in various macromolecular interactions during protein biosynthesis. To date, detailed understanding of the combined effects of more than one such modification has remained elusive. Here, the influence of modifications in the structural core of human mitochondrial $tRNA^{Lys}$ was investigated by smFRET. This technique allows following the folding process, starting from a largely unstructured conformation at very low salt conditions, passing through an extended cloverleaf structure, and ending in a functional L-shaped conformation at high salt concentrations. Individual contributions to the stability of the L-shaped conformation could be identified for 1-methyladenosine 9 (m^1A9), *N*2-methylguanosine 10 (m^2G10), and pseudouridines 27 and 28. While the pseudouridines unexpectedly displayed some unfavorable contributions in a structural equilibrium, m^2G alone did not show any appreciable effect at physiologically relevant ion concentrations. However, the stabilizing effect of m^1A9 was notably enhanced by m^2G10, demonstrating that these modifications act cooperatively in structuring the tRNA core. This observation presents a biophysical basis for the emerging notion that structural core modifications in tRNA act as a concerted network for the fine-tuning of structural features rather than as a binary all-or-nothing effect.

EXPERIMENTAL PROCEDURES

Preparation of Dye-Labeled Constructs

I CAC_dt^{Cy3}GUAAAGCUAACUUAGCAUUAACCUUUUAA
II CAC_dt^{Cy3}GUAAAGCUAACUUAGC
III GGUACCCAAAAUCACdt^{Cy3}GU
IVa AAm^{1}AGCUAACUUAGC
IVb AAAm^{2}GCUAACUUAGC
IVc AAm^{1}Am^{2}GCUAACUUAGC
Va AUUAACCUUUUAA
Vb pAΨΨAACCUUUUAA
VIa GUdt^{Cy5}AAAGAUUAAGAGAACCAACACCUCUUUACAGUGACCA-biotin
VIb GUdt^{Cy5}AAAGAUUAAGAGAGCCAACACCUCUUUACAGUGACCA-biotin

An overview of the employed oligonucleotides is given in Table 1. The RNA oligonucleotides IVa: AAm^{1}AGCUAACUUAGC, IVb: AAAm^{2}GCUAACUUAGC, IVc: AAm^{1}Am^{2}GCUAACUUAGC (m^1A = 1-methyladenosine, m^2G = 2-methylguanosine) were synthesized by solid-phase phosphoramidite chemistry employing the now commercially available 1-methyladenosine phosphoramidite (Glen Research) and the 2-methylguanosine phosphoramidite (Abeydeera and Chow, 2009; Höbartner et al., 2003). These were combined with fast deprotecting TAC amidites (Sigma-Aldrich) followed by the modified deprotection protocol as described (Mikhailov et al., 2002). 14 mer oligonucleotides containing both modifications could be isolated only in small amounts (about 1 OD_{260}) as a consequence of low coupling yield, which we obtained for the m^2G modification. Purification was accomplished by ion exchange chromatography on a Mono Q column with a perchlorate gradient (Bobkov et al., 2008), followed by reversed phase chromatography (X-Bridge C18). Characterization and analysis of the oligonucleotides were carried out by HPLC/MS (CapLC, Waters, and Q-Tof-2, Micromass, UK, respectively) (Bobkov et al., 2008). In the synthesis of RNA oligonucleotides I: CACdt^{Cy3}GUAAAGCUAACUUAGCAUUAACCUUUUAA, II: CAC_dt^{Cy3}GUAAAGCUAACUUAGC, III: GGUACCCAAAAUCACdt^{Cy3}GU, VI: GUdt^{Cy5}AAAGAUUAAGAGAACCAACACCUCUUUACAGUGACCA-biotin (all from IBA, Göttingen, Germany), 5′-dimethoxytrityl-5-[*N*-(trifluoroacetylaminohexyl)-3-acrylimido]-2′-deoxyuridine,3′-[(2-cyanoethyl)-(*N*,*N*-diisopropyl)]-phosphoramidite was coupled at sites denoted "dt" instead of uridine phosphoramidites, replacing uridine in the sequence with a 2′-deoxythymidine. It carries a linear 11-atom-chain spacer that ends in a primary amino group, to which NHS derivatives of Cy3 and Cy5 dyes were conjugated postsynthetically. The respective conjugation sites are indicated as dT^{Cy3} and dT^{Cy5}, respectively. RNA oligonucleotide Va: AUUAACCUUUUAA was also from IBA. RNA oligonucleotide Vb: pAΨΨAACCUUUUAA (p = 5′-phosphate) was obtained from Dharmacon (Lafayette, IN). Splint DNA GGGTGGGTCTGCTTGGTCACTGTAAAGAGGTGTTGGTTCTCTTAATCTTTAACTTAAAAGGTTAATGCTAAGTTAGCTTTACAGTGATTTTGGGTACC was from IBA.

Oligonucleotides synthesized without a 5′ monophosphate were phosphorylated by incubation with T4 polynucleotide kinase (T4-PNK, Fermentas, St. Leon-Rot, Germany) (0.75 U/μL) in KL buffer (50 mM Tris-HCl [pH 7.4], 10 mM $MgCl_2$), supplemented with 5 mM DTT and 2 mM ATP for 60 min at 37°C. The phosphorylated RNA was used immediately in enzymatic ligation or stored at –20°C until use.

Splint ligation was performed as follows: stoichiometric amounts of the various respective RNA fragments (2–8 μM) were hybridized to DNA template by heating to 75°C and slow cooling to room temperature over 10 min in KL buffer supplemented with 5 mM DTT and 2 mM ATP. T4 DNA ligase was added (2 U/μL) and ligation was carried out overnight at 16°C. Template DNA was removed by addition of 0.02–0.1 U/μL DNase I followed by 15 min incubation at 37°C. RNAs were purified by denaturing PAGE, eluted from the gel, and precipitated with ethanol. Concentrations were calculated from the absorption at 254 nm, as determined on a Nanodrop ND-1000 (Wilmington, DE)

spectrometer. The various tRNA derivatives synthesized are listed in Table 1, along with the respective oligoribonucleotides employed.

RNase P-RNA was obtained by in vitro transcription as described (Helm et al., 1998) (the corresponding plasmid was kindly provided by Prof. Roland Hartmann, Marburg). Preparative RNase P processing of all precursor constructs (suffix "pre-" in Table 1) was performed by incubation of tRNA-precursor (0.5–5 μM) with two equivalents of RNase P-RNA at 37°C for 90 min in RNP buffer (50 mM Tris-HCl [pH 7.6], 100 mM NH_4OAc, 100 mM $MgOAc_2$, 0.1 mM EDTA), followed by PAGE purification.

Single-Molecule FRET Measurements

Single-molecule experiments were carried out on ~100 pM freely diffusing FRET-labeled tRNA constructs. The buffer solution containing 50 mM Tris was supplemented with the appropriate amount of cations to achieve the desired concentrations in titration experiments. Also, ascorbic acid (1 mM) and methyl viologen (1 mM) were added to the sample solution, to reduce fluorophore blinking and bleaching (Vogelsang et al., 2008). For smFRET burst analysis measurements, droplets (~30 μl) of the probe solutions were deposited on microscope coverslips and kept under a water-saturated nitrogen atmosphere during measurements. smFRET measurements were conducted on a homemade multi-channel confocal microscope based on a Zeiss Axiovert 135 TV frame (Kobitski et al., 2008; Kuzmenkina et al., 2005; Rieger et al., 2010). Sample excitation and signal detection as well as raw data analysis were performed essentially as described (Rieger et al., 2010).

SUPPLEMENTAL INFORMATION

Supplemental Information includes three figures and one table and can be found with this article online at doi:10.1016/j.chembiol.2011.03.016.

ACKNOWLEDGMENTS

We thank Jeff Rozensky (Leuwen), N. Dinuka Abeydeera, and R. Varakala (Detroit) for technical assistance. This work was supported by the Volkswagen Foundation (VW-I/82549), the Deutsche Forschungsgemeinschaft (DFG) (HE 3397/3), and CFN.

Received: January 21, 2011
Revised: March 14, 2011
Accepted: March 29, 2011
Published: July 28, 2011

REFERENCES

Abeydeera, N.D., and Chow, C.S. (2009). Synthesis and characterization of modified nucleotides in the 970 hairpin loop of Escherichia coli 16S ribosomal RNA. Bioorg. Med. Chem. *17*, 5887–5893.

Alexandrov, A., Grayhack, E.J., and Phizicky, E.M. (2005). tRNA m7G methyltransferase Trm8p/Trm82p: evidence linking activity to a growth phenotype and implicating Trm82p in maintaining levels of active Trm8p. RNA *11*, 821–830.

Alexandrov, A., Chernyakov, I., Gu, W., Hiley, S.L., Hughes, T.R., Grayhack, E.J., and Phizicky, E.M. (2006). Rapid tRNA decay can result from lack of nonessential modifications. Mol. Cell *21*, 87–96.

Anderson, J., Phan, L., Cuesta, R., Carlson, B.A., Pak, M., Asano, K., Bjork, G.R., Tamame, M., and Hinnebusch, A.G. (1998). The essential Gcd10p-Gcd14p nuclear complex is required for 1-methyladenosine modification and maturation of initiator methionyl-tRNA. Genes Dev. *12*, 3650–3662.

Anderson, J., Phan, L., and Hinnebusch, A.G. (2000). The Gcd10p/Gcd14p complex is the essential two-subunit tRNA(1-methyladenosine) methyltransferase of Saccharomyces cerevisiae. Proc. Natl. Acad. Sci. USA *97*, 5173–5178.

Björk, G.R. (1995). Genetic dissection of synthesis and function of modified nucleosides in bacterial transfer RNA. Prog. Nucleic Acid Res. Mol. Biol. *50*, 263–338.

Bobkov, G.V., Mikhailov, S.N., Van Aerschot, A., and Herdewijn, P. (2008). Phosphoramidite building blocks for efficient incorporation of 2′-O-aminoethoxy(and propoxy)methyl-nucleosides into oligonucleotides. Tetrahedron *64*, 6238–6251.

Cantara, W.A., Crain, P.F., Rozenski, J., McCloskey, J.A., Harris, K.A., Zhang, X., Vendeix, F.A., Fabris, D., and Agris, P.F. (2011). The RNA modification database, RNAMDB: 2011 update. Nucleic Acids Res. *39*, D195–D201.

Chernyakov, I., Whipple, J.M., Kotelawala, L., Grayhack, E.J., and Phizicky, E.M. (2008). Degradation of several hypomodified mature tRNA species in Saccharomyces cerevisiae is mediated by Met22 and the 5′-3′ exonucleases Rat1 and Xrn1. Genes Dev. *22*, 1369–1380.

Czerwoniec, A., Dunin-Horkawicz, S., Purta, E., Kaminska, K.H., Kasprzak, J.M., Bujnicki, J.M., Grosjean, H., and Rother, K. (2009). MODOMICS: a database of RNA modification pathways. 2008 update. Nucleic Acids Res. *37*, D118–D121.

Derrick, W.B., and Horowitz, J. (1993). Probing structural differences between native and in vitro transcribed Escherichia coli valine transfer RNA: evidence for stable base modification-dependent conformers. Nucleic Acids Res. *21*, 4948–4953.

Engelke, D.R., and Hopper, A.K. (2006). Modified view of tRNA: stability amid sequence diversity. Mol. Cell *21*, 144–145.

Helm, M. (2006). Post-transcriptional nucleotide modification and alternative folding of RNA. Nucleic Acids Res. *34*, 721–733.

Helm, M., Brule, H., Degoul, F., Cepanec, C., Leroux, J.P., Giegé, R., and Florentz, C. (1998). The presence of modified nucleotides is required for cloverleaf folding of a human mitochondrial tRNA. Nucleic Acids Res. *26*, 1636–1643.

Helm, M., Giegé, R., and Florentz, C. (1999). A Watson-Crick base-pair-disrupting methyl group (m1A9) is sufficient for cloverleaf folding of human mitochondrial tRNALys. Biochemistry *38*, 13338–13346.

Helm, M., Kobitski, A., and Nienhaus, G.U. (2009). Single-molecule Förster resonance energy transfer studies of RNA structure, dynamics and function. Biophys. Rev. *1*, 161–176.

Hengesbach, M., Kobitski, A., Voigts-Hoffmann, F., Frauer, C., Nienhaus, G.U., and Helm, M. (2008). RNA intramolecular dynamics by single-molecule FRET. Curr. Protoc. Nucleic Acid Chem., Chapter 11, Unit 11.12.

Hengesbach, M., Voigts-Hoffmann, F., Hofmann, B., and Helm, M. (2010). Formation of a stalled early intermediate of pseudouridine synthesis monitored by real-time FRET. RNA *16*, 610–620.

Höbartner, C., Kreutz, C., Flecker, E., Ottenschlager, E., Pils, W., Grubmayr, K., and Micura, R. (2003). The synthesis of 2′-O-[(triisopropylsilyl)oxy] methyl (TOM) phosphoramidites of methylated ribonucleosides (m(1)G, m(2)G, m(2)(2)G, m(1)I, m(3)U, m(4)C, m(6)A, m(2)(6)A) for use in automated RNA solid-phase synthesis. Monatsh. Chem. *134*, 851–873.

Jackman, J.E., Montange, R.K., Malik, H.S., and Phizicky, E.M. (2003). Identification of the yeast gene encoding the tRNA m1G methyltransferase responsible for modification at position 9. RNA *9*, 574–585.

Juhling, F., Mörl, M., Hartmann, R.K., Sprinzl, M., Stadler, P.F., and Pütz, J. (2009). tRNAdb 2009: compilation of tRNA sequences and tRNA genes. Nucleic Acids Res. *37*, D159–D162.

Kadaba, S., Krueger, A., Trice, T., Krecic, A.M., Hinnebusch, A.G., and Anderson, J. (2004). Nuclear surveillance and degradation of hypomodified initiator tRNAMet in S. cerevisiae. Genes Dev. *18*, 1227–1240.

Kadaba, S., Wang, X., and Anderson, J.T. (2006). Nuclear RNA surveillance in Saccharomyces cerevisiae: Trf4p-dependent polyadenylation of nascent hypomethylated tRNA and an aberrant form of 5S rRNA. RNA *12*, 508–521.

Kapanidis, A.N., Lee, N.K., Laurence, T.A., Doose, S., Margeat, E., and Weiss, S. (2004). Fluorescence-aided molecule sorting: analysis of structure and interactions by alternating-laser excitation of single molecules. Proc. Natl. Acad. Sci. USA *101*, 8936–8941.

Kobitski, A.Y., Nierth, A., Helm, M., Jäschke, A., and Nienhaus, G.U. (2007). Mg2+-dependent folding of a Diels-Alderase ribozyme probed by single-molecule FRET analysis. Nucleic Acids Res. *35*, 2047–2059.

Kobitski, A.Y., Hengesbach, M., Helm, M., and Nienhaus, G.U. (2008). Sculpting an RNA conformational energy landscape by a methyl group modification–a single-molecule FRET study. Angew. Chem. Int. Ed. Engl. *47*, 4326–4330.

Kotelawala, L., Grayhack, E.J., and Phizicky, E.M. (2008). Identification of yeast tRNA Um(44) 2′-O-methyltransferase (Trm44) and demonstration of a Trm44 role in sustaining levels of specific tRNA(Ser) species. RNA *14*, 158–169.

Kurschat, W.C., Müller, J., Wombacher, R., and Helm, M. (2005). Optimizing splinted ligation of highly structured small RNAs. RNA *11*, 1909–1914.

Kuzmenkina, E.V., Heyes, C.D., and Nienhaus, G.U. (2005). Single-molecule Forster resonance energy transfer study of protein dynamics under denaturing conditions. Proc. Natl. Acad. Sci. USA *102*, 15471–15476.

Kuzmenkina, E.V., Heyes, C.D., and Nienhaus, G.U. (2006). Single-molecule FRET study of denaturant induced unfolding of RNase H. J. Mol. Biol. *357*, 313–324.

Madore, E., Florentz, C., Giegé, R., Sekine, S., Yokoyama, S., and Lapointe, J. (1999). Effect of modified nucleotides on Escherichia coli tRNAGlu structure and on its aminoacylation by glutamyl-tRNA synthetase. Predominant and distinct roles of the mnm5 and s2 modifications of U34. Eur. J. Biochem. *266*, 1128–1135.

Messmer, M., Gaudry, A., Sissler, M., and Florentz, C. (2009a). Pathology-related mutation A7526G (A9G) helps in the understanding of the 3D structural core of human mitochondrial tRNA(Asp). RNA *15*, 1462–1468.

Messmer, M., Pütz, J., Suzuki, T., Sauter, C., Sissler, M., and Catherine, F. (2009b). Tertiary network in mammalian mitochondrial tRNAAsp revealed by solution probing and phylogeny. Nucleic Acids Res. *37*, 6881–6895.

Micura, R., Pils, W., Höbartner, C., Grubmayr, K., Ebert, M.O., and Jaun, B. (2001). Methylation of the nucleobases in RNA oligonucleotides mediates duplex-hairpin conversion. Nucleic Acids Res. *29*, 3997–4005.

Mikhailov, S.N., Rozenski, J., Efimtseva, E.V., Busson, R., Van Aerschot, A., and Herdewijn, P. (2002). Chemical incorporation of 1-methyladenosine into oligonucleotides. Nucleic Acids Res. *30*, 1124–1131.

Motorin, Y., and Helm, M. (2010). tRNA stabilization by modified nucleotides. Biochemistry *49*, 4934–4944.

Perret, V., Garcia, A., Puglisi, J., Grosjean, H., Ebel, J.P., Florentz, C., and Giegé, R. (1990). Conformation in solution of yeast tRNA(Asp) transcripts deprived of modified nucleotides. Biochimie *72*, 735–743.

Pütz, J., Florentz, C., Benseler, F., and Giegé, R. (1994). A single methyl group prevents the mischarging of a tRNA. Nat. Struct. Biol. *1*, 580–582.

Rieger, R., Kobitski, A., Sielaff, H., and Nienhaus, G.U. (2010). Evidence of a Folding Intermediate in RNase H from Single-Molecule FRET Experiments. Chemphyschem. *12*, 627–633.

Rife, J.P., Cheng, C.S., Moore, P.B., and Strobel, S.A. (1998). N 2-methylguanosine is iso-energetic with guanosine in RNA duplexes and GNRA tetraloops. Nucleic Acids Res. *26*, 3640–3644.

Sampson, J.R., and Uhlenbeck, O.C. (1988). Biochemical and physical characterization of an unmodified yeast phenylalanine transfer RNA transcribed in vitro. Proc. Natl. Acad. Sci. USA *85*, 1033–1037.

Shi, H., and Moore, P.B. (2000). The crystal structure of yeast phenylalanine tRNA at 1.93 A resolution: a classic structure revisited. RNA *6*, 1091–1105.

Vogelsang, J., Kasper, R., Steinhauer, C., Person, B., Heilemann, M., Sauer, M., and Tinnefeld, P. (2008). A reducing and oxidizing system minimizes photobleaching and blinking of fluorescent dyes. Angew. Chem. Int. Ed. Engl. *47*, 5465–5469.

Voigts-Hoffmann, F., Hengesbach, M., Kobitski, A.Y., van Aerschot, A., Herdewijn, P., Nienhaus, G.U., and Helm, M. (2007). A methyl group controls conformational equilibrium in human mitochondrial tRNA(Lys). J. Am. Chem. Soc. *129*, 13382–13383.

